INTERNATIONAL JOURNAL OF PRECISION ENGINEERING AND MANUFACTURING Vol. 16, No. 2, pp. 343-350 FEBRUARY 2015 / 343
DOI: 10.1007/s12541-015-0045-x

Quasi-Steady-State Scheme and Application on Prewhirl Flow and Heat Transfer in Aeroengine

Hong Xiao[1], Zhe-Zhu Xu[2], and Sung-Ki Lyu[2,#]

1 School of Power and Energy, Northwestern Polytechnical University, Xi'an, 710-072, China
2 School of Mechanical and Aerospace Engineering, ReCAPT, Gyeongsang National University, 63, Gajwa-gil 29beon-gil, Jinju-si, Gyeongsangnam-do, 660-701, South Korea
Corresponding Author / E-mail: sklyu@gnu.ac.kr, TEL: +82-55-772-1632, FAX: +82-55-772-1578

KEYWORDS: Quasi-steady-state scheme, Unsteady flow, Prewhirl flow, Turbine disc cavity, Aeroengine

For solving three-dimensional complex unsteady flow to predict aerodynamic characteristics of turbine disc cavity in aeroengine, a quasi-steady-state scheme is proposed. To validate and get reliable turbulence model, three-dimensional numerical studies, of turbine disc cavity prewhirl flow and heat transfer, are conducted. For comparison, unsteady state computational fluid dynamics simulations of prewhirl flow are also performed. Five turbulence models, including standard k-å model, RNG k-å model, Realizable k-å model, SST k-ù model and RSM model, are applied both quasi-steady-state scheme and unsteady CFD. Then, reliable quasi-steady-state scheme is obtained and the feasibility, instead of unsteady-state CFD simulation for reducing time resource, is verified. Furthermore, investigations of prewhirl flow and heat transfer in turbine disc cavity of aeroengine are conducted by the proposed quasi-steady-state scheme. It was found that the rotation Reynolds number should be increased to strengthen the blade cooling and weaken the heat transfer in turbine disc cavity. All the results are applied in the design of aeroengine. Also, it proves that quasi-steady-state scheme is effective in the prediction of aerodynamic characteristics in aeroengine.

Manuscript received: October 12, 2014 / Revised: October 23, 2014 / Accepted: November 10, 2014

1. Introduction

In the past decades, turbine disc cavity flow with prewhirl nozzle has been studied extensively since it plays an important role in the aero engine systems. In the turbine disc cavity, numerous structure and flow parameters may affect its aerodynamic characteristics. Then, the most important work in this field is how to find the impacted parameters and its correlations. And so, analysis theories and numerical schemes are extensively studied in the past decades. Firstly, Hasan karabay[1,2] proposed a simple analysis theory for prewhirl flow and studied the impacted parameters on prewhirl cavity which included velocity, pressure and Nussle number. Then, Robert Pilbrow[3] presenteda few correlations between common swirl ratio and temperature drop based on the studies of different structures and gas flow parameters. Latter, Robert Pilbrow found that that the pressure coefficient and Nussle number were greatly depended on only a few structure and flow parameters. Contemporaneously, Ma.F.Gord[4] executed steady-state numerical study for prewhirl flow on disc cavity in which the pressure loss was found to be agreed very well with experiment but the local Nussle number was not. Latter, the effect of different direct-transfer system structures on the flow coefficient were also studied by T. Geis and M. Dittmann.[5,6] Although numerous tudies have been conducted, the numerical study of prewhirl flow in turbine disc cavity is still in the face of challenges because the time resource is huge[7-9] for the strong unsteady gas flow. Therefore, for reducing the time resource and get unsteady simulation, the simplified or approximated unsteady schemes still been of interesting in the numerical study of prewhirl flow on turbine disc cavity in aeroengine.[10,11]

Computational fluid dynamics (CFD) play an important role in the design and manufacture,[12-14] but the time resource of unsteady-state CFD is huge and it is not suitable for some engineering cases. The present study developed a new approximated unsteady method named by quasi-steady-state scheme to reduce time resource with keeping the level of precision. And also, for validation, the studies of prewhirl flow and heat transfer in turbine disc cavity were performed.

Then, investigations of prewhirl flow and heat transfer in turbine disc cavity of aeroengine are conducted by the quasi-steady-state scheme.

2. Physical System

Fig. 1 presents the typical three-dimensional prewhirl flow of

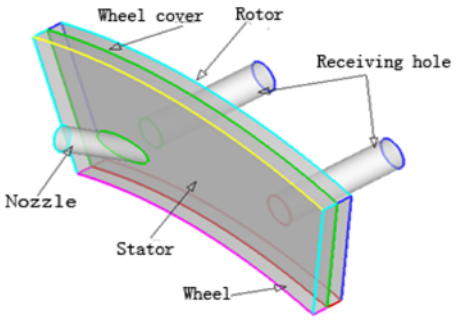

Fig. 1 The physical system of three-dimensional prewhirl flow

turbine disc cavity in aeroengine. As seen in Fig. 1, gas flow enters a cavity through stationary nozzles and then move into a rotational disc cavity crossing rotational receiving holes. This system changes the gas flow from station to rotation and transforms it to cooling medium and so we usually name it by the prewhirl system.

3. Numerical Methods

3.1 Governed equations

As mentioned in Part. 1, the prewhirl system is a rotating frame, so the standard incompressible Navier-Stokes equations can not be used directly in the simulation. And, an additional force term should be implemented in the momentum equation. In the following, we expressed the incompressible N-S equations for the rotating coordinate system,

$$\nabla \bullet \vec{v} = 0 \tag{1}$$

$$\rho(\vec{v}\nabla)\vec{v} = -\nabla p_{eff} + (\mu+\mu_t)\nabla^2\vec{v} - \rho(2\vec{\omega}\times\vec{v} + \vec{\omega}\times\vec{\omega}\times\vec{r}) \tag{2}$$

$$\rho c_p(\vec{v}\bullet\nabla T) = (\lambda+\lambda_t)\nabla^2 T \tag{3}$$

And also, the following hypothesizes are implanted for solving governed Eqs. (1)~(3),

1) The gravitational force is ignored.

2) The thermal conductivity, viscosity coefficient and specific heat ratio are retained in constant.

3) We only consider convection and diffusion heat transfer term in the energy equation. The heating of energy dissipation and the energy exchange resulting from $\vec{v}\bullet\nabla p$ item are negligible.

4) p_{eff}, in momentum equation, is the combination pressure value, which includes two static pressure and pulsation kinetic-energy

For the convenience of the results analysis, we transferred the governed equations into dimensionless forms by using the following dimensional variables.

(1) The rotary table radius b is used for the characteristic scale.

(2) The cold air inlet velocity v_0 are used to define the dimensionless velocity.

(3) The dimensionless physical parameters are defined by inlet parameters (ρ_{in}, μ_{in}, λ_{in}, cp_{in}).

(4) Excess temperature θ is defined as T-T_0 and so the characteristic temperature drop θ_w is taken as characteristic temperature, which is equal to $q_w d/\lambda$.

$$\vec{x} = \frac{\vec{r}}{b},\ G = \frac{s}{b},\ \vec{V} = \frac{\vec{v}}{v_0},\ \Theta = \frac{\theta}{\theta_w},\ P = \frac{p}{\rho v_0^2}$$

Dimensionless operator is also expressed as,

$$\vec{\nabla} = \frac{\nabla}{d}$$

And also, $\omega = \omega\vec{k}$ is resulted from the rotating axis z-axis.

Then, the dimensionless governed equations can be written as,

$$\nabla \bullet \vec{V} = 0 \tag{4}$$

$$(\vec{V}\bullet\nabla)\vec{V} = -\nabla P + \frac{1}{Re}(1+\mu_t)\nabla^2\vec{V} - \left(\frac{1}{Ro}\right)(2\vec{k}\times\vec{V}) + \frac{Gr_\omega}{Re^2}\left(Ro\left(\frac{d}{r_0}\right)(2\vec{k}\times\vec{V}) + (\vec{k}\times\vec{k}\times\vec{R})\right)\Theta \tag{5}$$

$$(\nabla\bullet\vec{V}\Theta) = \frac{1}{RePr}(1+\mu_t)\nabla^2\Theta \tag{6}$$

Here, Reynolds number, Rossby number, the rotating Reynolds number, Pr number, Rotating grashof number, and the Geometric dimensionless rate are defined as,

$$Re = \rho v_0 d/\mu$$

$$Ro = v_0/\omega d$$

$$Re_\omega = \rho w d^2/\mu$$

$$Pr = \mu c_p/\lambda$$

$$Gr\omega = \frac{\gamma\omega^2 r_0^4 \Delta T}{\nu^2}$$

$$\frac{r_m}{b}$$

3.2 Near wall treatment

In the present study, for the comparison, five turbulence models, including the standard k-ε, RNG k-ε, Realizable k-ε, SST k-ω, RSM, are applied in the solving conservation laws. The near-wall model and wall function method are usually implemented for the treating solid wall. In near-wall model, turbulent model is corrected so that the wall region affected by the viscous force can also be solved by the mesh generation. However, a limitation of such an approach is the sensitivity of the results to the selection of the power-law exponent. Dynamic tuning based on the local ow conditions (turbulence levels, pressure gradients) may improve the range of applicability.[15,16] But, for the present high-Reynolds number flow, in the region which is affected by near-wall viscous forces, variables change rapidly that it do not need to be solved. Although for the assumption of standard profiles which have insignificant theoretical foundation in non-equilibrium flow, particularly near flow-separation and impingement points, the wall function method have been criticized. A second undesirable restriction has been the need

to locate the near-wall node in the fully-turbulent region - a requirement that limits grid refinement. Recently, the wall function method have been revitalized though the "analytical wall function" approach.[17,18] For smooth wall boundary layers, it goes a way to meeting the criteria; namely, better behavior in non-equilibrium boundary layers and insensitivity to the sizes of near wall cell.[19] So, the new wall function is selected in the treating solid wall region for saving computation resources.

3.3 Algorithm

The finite volume method and SIMPLE algorithm are applied in the present study. In the SIMPLE algorithm, firstly, the velocity field is obtained by the momentum equation with the given constant pressure field which can be the assumed value or the value of the last iteration. Since that the pressure field is assumed or inaccurate, the obtained velocity field normally does not satisfy the mass equation. So, the pressure field must be modified again. The principle of modification is that the velocity field corresponding to the modified pressure field should satisfy the mass conservation equation in this iteration level. Then, we get the corrected pressure by the substitution of the relationship between pressure and speed regulated by the discrete form of the mass equation. Furthermore, the new velocity field is got according to the modified pressure field. And then, the convergence of the velocity field is checked. If not, the corrected pressure value is applied in the calculation of next level as the given pressure field till a converged solution is obtained.

3.4 Boundary condition

In the present study, the calculation domain contains the inlet, outlet and solid wall boundary conditions. The treatments of boundary conditions are present as follows.

1) Inlet boundary conditions: $U=U_{in}$, $V=V_{in}$, $W=W_{in}$, $k=k_{in}$, $\varepsilon=\varepsilon_{in}$.

2) The pressure outlet boundary conditions are applied and the static pressure of the outlet is set to 1 atm.

3) In the wall boundary conditions, the solid walls are divided into two different conditions including static and rotating wall surfaces. On the joint surface of fluid and solid, the no-shift is set as static wall: $U=V=W=k=0$, $\partial\varepsilon=\partial n=0$, $\partial p=\partial n=0$ (n is the normal direction of the solid wall) and rotating wall: $U=V=k=0$, $W=\Omega r$, $\partial\varepsilon=\partial n=0$, $\partial p=\partial n=0$.

4) For the thermal boundary conditions, static plate wall, internal screens and external screens are taken as insulation screen. The heat flux of given rotating disc wall is constant and set as, q=5000 w/m^2. And, the temperature of air inlet is set as 300 K.

4. Result

4.1 Calculation process

For saving time resource, we select one-twelfth of the disc cavity to create the three-dimensional calculation domain as its symmetric structure, as shown in Fig. 1. The outer diameter of disc cavity is 250 mm, with height 46.8 mm, axial clearance 10 mm, radial position of prewhirl nozzle 221.7 mm, diameter of nozzle 8 mm, prewhirl angle 20°, radial position of receiving hole 220 mm, diameter of receiving hole 10mm, and length/diameter of receiving hole 4.

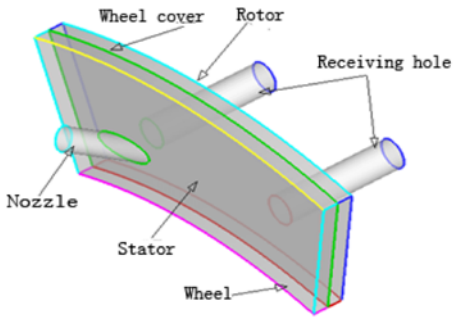

Fig. 2 Three-dimensional geometric models

As its rotation, the gas flow that drains into single blade is always shifting. It results in the periodic thermal load and causes an adverse influence on the blade life. In this system, the total pressure of inlet for blade cooling channel should be large enough so that it cannot results in the heat reflux. And also, the pressure loss is required to be small in the prewhirl disc cavity system.

The most important characteristic parameter is flow coefficient which is defined as the ratio of actual flow and isentropic flow and be used to characterize the capability of air flow. Dimensionless temperature difference is defined as,

$$\Delta T=\frac{(T_0-T_{trl,2})}{(\omega r_b)^2} \tag{7}$$

Here, T_0 is the total temperature of system inlet. $T_{trl,2}$ is the relative total temperature of receiving hole inlet based on relative coordinate system. ω is rotation speed and r_b is radial position of receiving hole. And,

$$\frac{T_{rel,t2}}{T_{t2}}=1+\frac{u^2-2uc_{t2}}{2c_pT_{t2}} \tag{8}$$

$$\frac{P_{rel,t2}}{P_{t2}}=\left(1+\frac{u^2-2uc_{t2}}{2c_pT_{t2}}\right)^{\frac{k}{k-1}} \tag{9}$$

where, u is rotation speed. c_p is specific heat at constant pressure. T_2 is the total temperature of receiving hole inlet based on absolute coordinate system. And, c_{t2} is tangential speed of receiving hole based on absolute coordinate system.

Pressure loss coefficient is expressed as

$$\zeta=\frac{(P_0-P_{t,2})}{\frac{1}{2}\rho_0\Omega^2r_e^2}$$

Here, P_0 is total pressure at system inlet. P_{t2} is total pressure at receiving hole inlet based on absolute coordinate system. ρ_0 is air density and r_e is radial position of prewhirl nozzle.

And, Flow coefficient of nozzle is defined as

$$C_{DN}=\frac{\dot{m}}{\frac{A_NP_0}{\sqrt{RT_0}}\sqrt{\frac{2k}{k-1}\left(\left(\frac{P_{1s}}{P_0}\right)^{\frac{2}{k}}-\left(\frac{P_{1s}}{P_0}\right)^{\frac{1+k}{k}}\right)}}$$

Furthermore, flow coefficient of receiving hole is expressed as

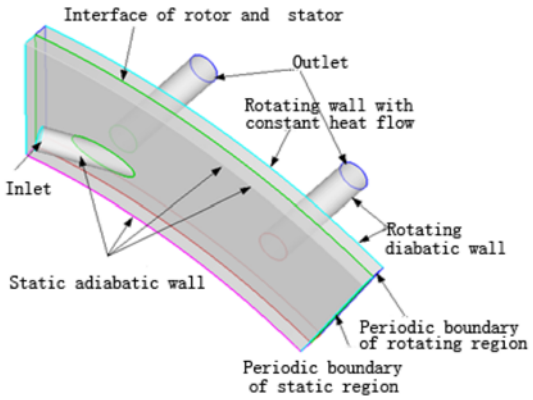

Fig. 3 Boundary conditions in the prewhirl disc cavity system

$$C_{DR}=\frac{\dot{m}}{\frac{A_R P_{rel,t2}}{\sqrt{RT_{rel,t2}}}\sqrt{\frac{2k}{k-1}\left(\left(\frac{P_{3s}}{P_{rel,t2}}\right)^{\frac{2}{k}}-\left(\frac{P_{3s}}{P_{rel,t2}}\right)^{\frac{1+k}{k}}\right)}}$$

And, flow coefficient of prewhirl system is defined as

$$C_D=\frac{\dot{m}}{\frac{A_N P_0}{\sqrt{RT_0}}\sqrt{\frac{2k}{k-1}\left(\left(\frac{P_{3s}}{P_0}\right)^{\frac{2}{k}}-\left(\frac{P_{3s}}{P_0}\right)^{\frac{1+k}{k}}\right)}}$$

Here, A_N is nozzle area. A_R is receiving hole area. $P_{rel,t2}$ is total pressure at receiving hole inlet in relative coordinate system. P_{1s} is static pressure of nozzle outlet and P_{3s} is static pressure at receiving hole outlet.

As shown in Fig. 3, for comparisons, we use several non-dimension parameters. These include dimensionless inlet flow C_w=4.16E4 ($\dot{m}$ = 0.192 kg/s), inlet total temperature T=300 K, rotation Reynolds number Re_ω=1.06E6 (Ω=7000 rpm). To obtain appropriate turbulence models, we compared the results of five turbulence models including standard k-ε, RNG k-ε, Realizable k-ε, SST k-ω and RSM in unsteady-state CFD and the proposed quasi-steady-state calculation.

4.2 Results

4.2.1 Unsteady-sate CFD result

In Fig. 4, we present the mass flow of specific receiving hole which is got from different turbulence model with angular phase of relative prewhirl nozzle in the receiving hole. It can be seen that the results of Realizable k-ε, SST k-ω, RSM are consistent with sine variation rule. And, the mass flow of receiving hole reaches a maximum when receiving hole and prewhirl nozzle is 0° and drops to the minimum at 15°. Meanwhile, the result of standard k-ε turbulence model is more consistent with sine (cosine) variation rule in positive relative angular phase area, but Realizable k-ε turbulence model value is unstable. In the real working process, when turntable rotates steadily, the mass flow through a receiving hole should be changed with the sine (cosine) function with relative position. On the other words, these two turbulence models are effective in the simulation of the prewhirl disc cavity system.

We present the results of dimensionless temperature difference in Fig. 5. It is observed that the results of RSM and SST k-ω were satisfied

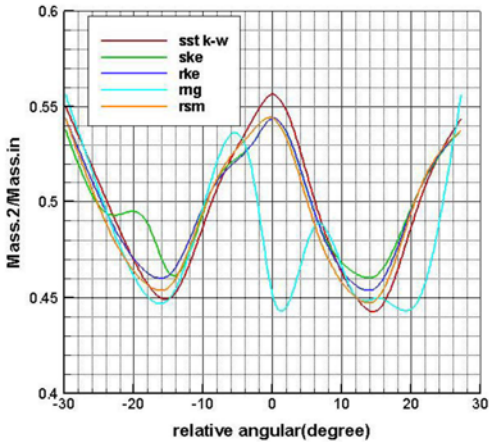

Fig. 4 Change curve of relative flow with relative angular phase in different turbulence models

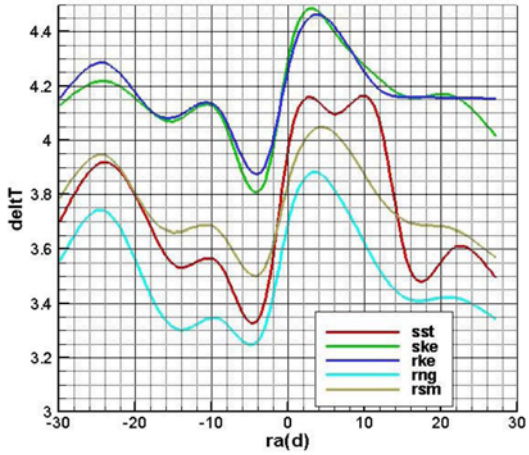

Fig. 5 Change curve of dimensionless temperature drop with relative angular phase in different turbulence models

with sine function but SST k-ω distribution is not regular.

Also, it can be found that the difference of the maximum and minimum is in 0.55 and the peak value on both sides of relative angular phase is 0°. This indicates that distribution of temperature drop through disc cavity is not completely determined by mass flow, and it is also governed by air-flow in disc cavity. Comparing of the results of SST k-ω and RSM, it can be seen that dimensionless temperature difference is increasing with mass flow. Unfortunately, the realizable k-ε model cannot predicate this trend and it present the obviously difference, so it is inadvisable in following study. Then, it can be concluded that the RSM turbulence model is a more reliable model for unsteady-state CFD.

The results of the flow coefficient and dimensionless pressure loss are shown in Figs. 6-7. It can be seen that, for all the results of flow coefficient except for the RNG k-ε model, variation rule is in good accordance. When relative angular phase is in 7.5, flow coefficient drops into a minimum and reaches a maximum in 15. Also, it can be observed that sine feature of dimensionless pressure drop is not obviously, and when relative phase angle is in 1°, dimensionless pressure drop is the smallest, with the smallest pressure loss at this time. This distribution

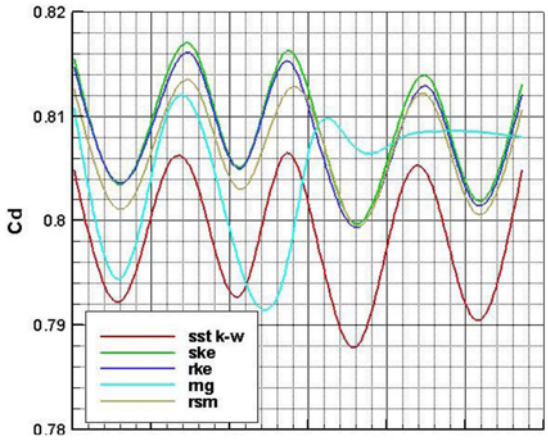

Fig. 6 Change curve of flow coefficient with relative angular phase in different turbulence models

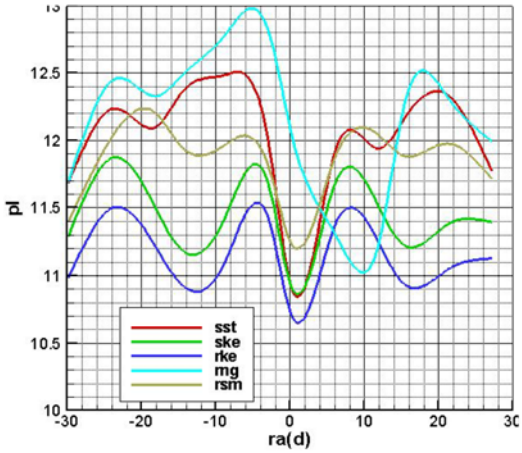

Fig. 7 Change curve of dimensionless pressure drop with relative angular phase in different turbulence models

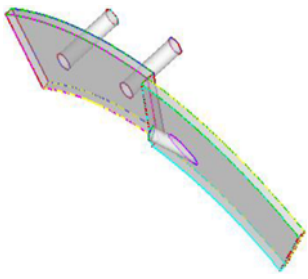

Fig. 8 Relative angular phase -30°

regulation is related to the air-flow in disc cavity to a great extent. Fig. 7 also shows that the dimensionless pressure drops with the relative angular phase in different turbulence models.

4.2.2 Quasi-steady-state result

In unsteady-sate CFD simulation, the time resource of RNG k-ε is the largest in the five turbulence models. The purpose of the present study is to find a new method for saving time resource in the prewhirl gas flow simulation Therefore, the RNG k-ε is not considered in quasi-steady-state simulation and we only compare unsteady-state standard k-ε, Realizable k-ε, SST k-ω and RSM models. Due to the main idea of quasi-steady-state simulation, it is necessary to creat different relative

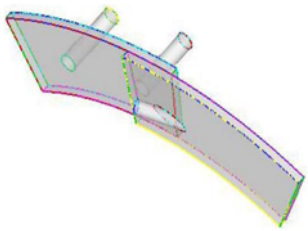

Fig. 9 Relative angular phase -22.5°

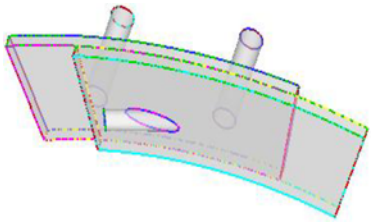

Fig. 10 Relative angular phase -15°

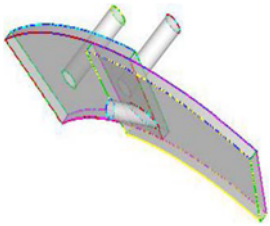

Fig. 11 Relative angular phase -7.5°

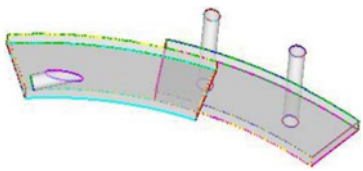

Fig. 12 Relative angular phase 7.5°

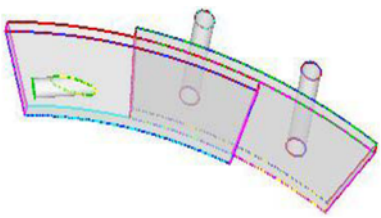

Fig. 13 Relative angular phase 15°

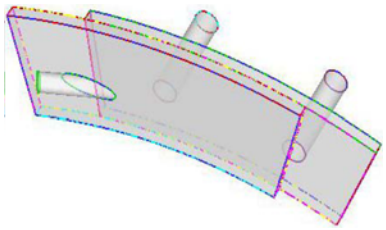

Fig. 14 Relative angular phase 22.5°

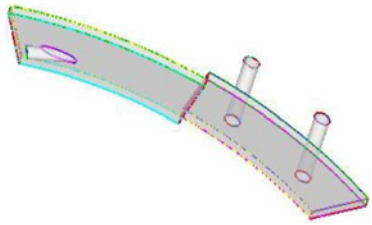

Fig. 15 Relative angular phase 30°

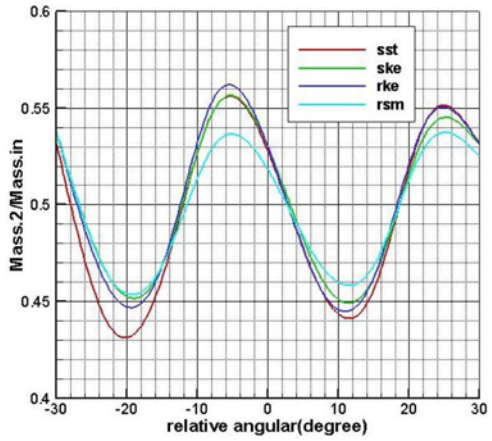

Fig. 16 Change curve of relative mass flow with relative angular phase in different turbulence models

positions for rotating and static areas. Therefore, we create 8 relative positions (see in Figs. 8~15) to correspond with relative angular phase specified by unsteady-state analysis.

The results of relative flow, dimensionless temperature drop, flow coefficient and dimensionless pressure drop are shown in Figs. 16~19. And, all these results are got from different turbulence model with relative angular phase. It can be observed that the relative mass got from four turbulence model with relative position shows sine (cosine) trends, and the result of RSM turbulence model is more in accordance with sine (cosine) distribution regulation. Therefore, RSM turbulence model is the best model for quasi-steady state. Also, the time resource is reduced by 10 times for one case compared with unsteady-sate CFD simulation.

5. Application

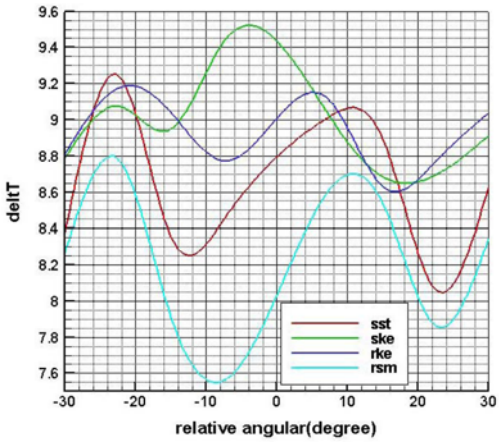

Fig. 17 Change curve of dimensionless temperature drop with relative angular phase in different turbulence models

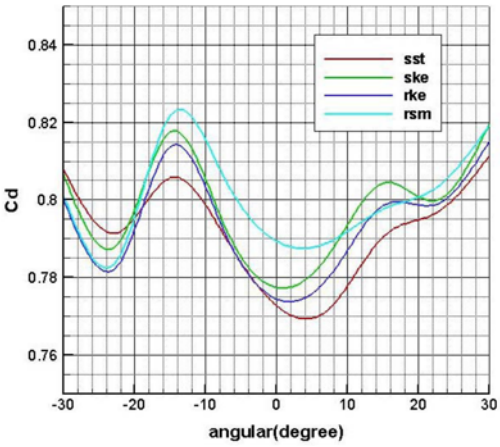

Fig. 18 Change curve of flow coefficient with relative angular phase in different turbulence models

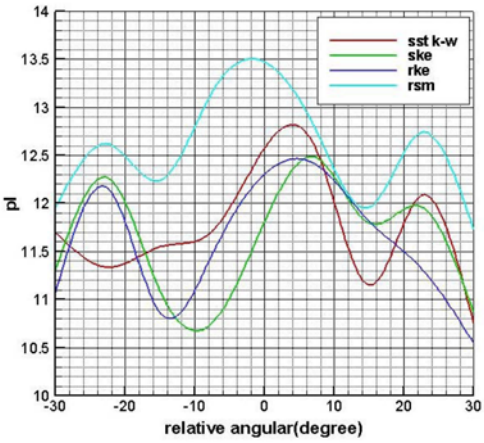

Fig. 19 Change curve of dimensionless pressure drop with relative angular phase in different turbulence models

For studying the impact of parameter Re_w, quasi-steady-state simulation are conducted in the prewhirl flow and heat transfer in aeroengine. Fig.

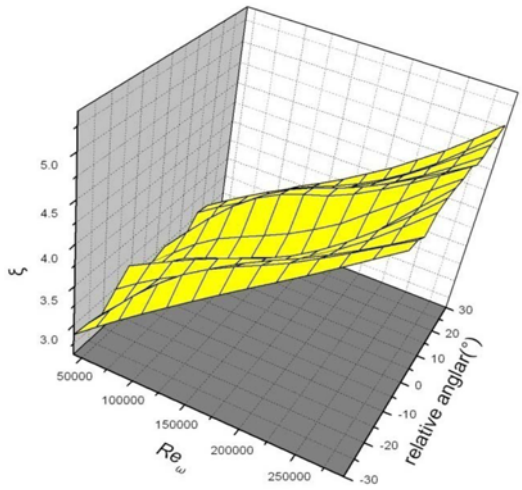

Fig. 20 Changing curve of ξ, with relative phase of prewhirl nozzle outlet and receiving hole 2 inlet

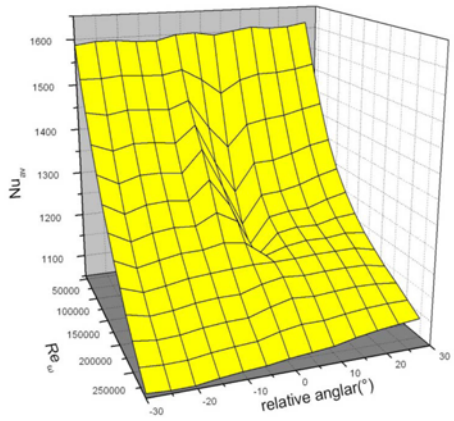

Fig. 21 Changing curve of Nu_{av}, with relative phase of prewhirl nozzle outlet and receiving hole 2 inlet

20 shows the temperature drop ξ, with the switch of phase difference under different Re_w. The temperature drop ξ, is increasing with Re_w, and concussion amplitude of ξ decreases, and when Re_w is 2.92e5. ξ presents in linear relations with the phase difference, except for existing minimum value when phase difference is 10°. On the contrary that Fig. 21 shows that Nu_{av} decreases with increasing of Re_w.

The impact of parameter on turbine disc cavity flow and heat transfer are also studied by the proposed quasi-steady-state simulation by changing dimensionless mass flow C_w and rotation Reynolds number Re_w. Numerical calculating results indicates that total pressure loss of system increases with increasing of C_w, and decreases with increasing of Re_w. Increasing of C_w or Re_w strengthens the effect on blade cooling, and heat transfer of turntable decreases with strengthening of cooling effect. All the results are applied in the design of aeroengine.

6. Conclusion

The present study propose a quasi-steady-state scheme for solving three-dimensional complex unsteady flow to predict aerodynamic characteristics of turbine disc cavity in aeroengine. For validation, unsteady-state computational fluid dynamics simulations (unsteady-state CFD) of prewhirl flow with five turbulence model are also performed. In unsteady-state CFD, the results of dimensionless temperature difference in RSM and SST k-ù were satisfied with sine function but SST k-ù distribution is not regular. And, the difference of the maximum and minimum is in 0.55 and the peak value on both sides of relative angular phase is 0°.In the quasi-steady-state study, all the results of relative flow, dimensionless temperature drop, flow coefficient and dimensionless pressure drop are got from different turbulence model with relative angular phase. Although that the relative mass got from four turbulence model with relative position shows sine (cosine) trends, the result of RSM turbulence model is more in accordance with sine (cosine) distribution regulation. Therefore, RSM turbulence model is regarded as the best model for quasi-steady state. Then, reliable quasi-steady-state scheme is obtained and the feasibility, instead of unsteady-state CFD simulation for reducing time resource, is verified. Also, the time resource is reduced by 10 times for the proposed quasi-steady-state scheme compared with unsteady-sate CFD simulation. Then, extensive cases of prewhirl flow in turbine disc cavity are considered and analyzed by the quasi-steady-state scheme. It was found that increasing of C_w or Re_w strengthens the effect on blade cooling, and heat transfer of turntable decreases with strengthening of cooling effect. All the results are applied in the design of aeroengine.

ACKNOWLEDGEMENT

This study was supported by Basic Science Research Program through the National Research Foundation of Korea (NRF) funded by the Ministry of Education, Science and Technology (NRF-2013R1A1A2058580). And the authors of Dr. Hong Xiao and Dr. Zhe-zhu Xu contributed equally to this work.

REFERENCES

1. Karabay, H., Wilson, M., and Owen, J. M., "Approximate Solutions for Flow and Heat Transfer in Pre-Swirl Rotating-Disc Systems," Proc. of ASME, Vol. 3, Paper No. 2001-GT-0200, 2001.
2. Karabay, H., Wilson, M., and Owen, J. M., "Predictions of Effect of Swirl on Flow and Heat Transfer in a Rotating Cavity," International Journal of Heat and Fluid Flow, Vol. 22, No. 2, pp. 143-155, 2001.
3. Karabay, H., Pilbrow, R., Wilson, M., and Owen, J. M., "Performance of Pre-Swirl Rotating-Disc Systems," Journal of Engineering for Gas Turbines and Power, Vol. 122, No. 3, pp. 442-450, 2000.
4. Smout, P. D., Chew, J. W., and Childs, P. R., "Icas-GT: A European Collaborative Research Programme on Internal Cooling Air Systems for Gas Turbines," Proc. of ASME Turbo Expo, Vol. 3, pp. 907-914, 2002.
5. Young, C., "Fluid Flow and Heat Transfer within the Rotating

Internal Cooling Air Systems of Gas Turbines," The Brite Euram ICAS-GT Program during 1998-2000. Vol. 2, pp. 1-19, 2000.

6. Farzaneh-Gord, M., "Heat Transfer Over Rotor Surface in a Pre-Swirl Rotating-Disc System," International Journal of Dynamics of Fluids, Vol. 3, No. 1, p. 81, 2007.
7. Geis, T., Dittmann, M., and Dullenkopf, K., "Cooling Air Temperature Reduction in a Direct Transfer Preswirl System," Proc. of ASME Turbo Expo, Vol. 5, pp. 955-964, 2003.
8. Dittmann, M., Geis, T., Schramm, V., Kim, S., and Witting, S., "Discharge Coefficients of a Pre-swirl System in Secondary Air Systems," Proc. of ASME Turbo Expo, Vol. 3, Paper No. 2001-GT-0122, 2001.
9. Faboi, C., Nicholas, J. H., John, W. C., and Timothy, S., "Unsteady Numerical Simulation of the Flow in a Direct Transfer Pre-swirl System," Proc. of ASME Turbo Expo, Vol. 4, pp. 1647-1655, 2008.
10. Snowsill, G. D. and Young, C., "Application of CFD to Assess the Performance of a Novel Pre-Swirl Configuration," Proc. of ASME Turbo Expo, Vol. 4, pp. 1555-1562, 2008.
11. Snowsill, G. D. and Young, C., "The Application of CFD to Underpin the Design of Gas Turbine Pre-swirl Systems," Proc. of ASME Turbo Expo, Vol. 3, pp. 1393-1401, 2006.
12. Kang, T. J. and Park, W. G., "Numerical Investigation of Active Control for an S809 Wind Turbine Airfoil," Int. J. Precis. Eng. Manuf., Vol. 14, No. 6, pp. 1037-1041, 2013.
13. Yoon, S. H., Lim, H. C., and Kim, D. K., "Study of Several Design Parameters on Multi-Blade Vertical Axis Wind Turbine," Int. J. Precis. Eng. Manuf., Vol. 14, No. 5, pp. 831-837, 2013.
14. Kwak, Y. K., Kim, S. H., and Ahn, J. H., "Improvement of Positioning Accuracy of Magnetostrictive Actuator by Means of Built-in Air Cooling and Temperature Control," Int. J. Precis. Eng. Manuf., Vol. 12, No. 5, pp. 829-834, 2011.
15. Choi, J. I., Oberoi, R. C., Edwards, J. R., and Rosati, J. A., "An Immersed Boundary Method for Complex Incompressible Flows," Journal of Computational Physics, Vol. 224, No. 2, pp. 757-784, 2007.
16. Posa, A. and Balaras, E., "Model-based Near-Wall Reconstructions for Immersed-Boundary Methods," Theoretical and Computational Fluid Dynamics, Vol. 28, pp. 473-483, 2014.
17. Craft, T. J., Gerasimov, A. V., Iacovides, H., and Launder, B. E., "Progress in the Generalization of Wall-Function Treatments," International Journal of Heat and Fluid Flow, Vol. 23, No. 2, pp. 148-160, 2002.
18. Craft, T. J., Gerasimov, A. V., Iacovides, H., Kidger, J. W., and Launder, B. E., "The Negatively Buoyant Turbulent Wall Jet: Performance of Alternative Options in RANS Modelling," International Journal of Heat and Fluid Flow, Vol. 25, No. 5, pp. 809-823, 2004.
19. Apsley, D., "CFD Calculation of Turbulent Flow with Arbitrary Wall Roughness," Flow, Turbulence and Combustion, Vol. 78, No. 2, pp. 153-175, 2007.